

On Suppressing Range of Adaptive Stepsizes of Adam to Improve Generalisation Performance

Guoqiang Zhang

Abstract—A number of recent adaptive optimizers improve the generalisation performance of Adam by essentially reducing the variance of adaptive stepsizes to get closer to SGD with momentum. Following the above motivation, we suppress the range of the adaptive stepsizes of Adam by exploiting the layerwise gradient statistics. In particular, at each iteration, we propose to perform three consecutive operations on the second momentum v_t before using it to update a DNN model: (1): down-scaling, (2): ϵ -embedding, and (3): down-translating. The resulting algorithm is referred to as SET-Adam, where SET is a brief notation of the three operations. The down-scaling operation on v_t is performed layerwise by making use of the angles between the layerwise subvectors of v_t and the corresponding all-one subvectors. Extensive experimental results show that SET-Adam outperforms eight adaptive optimizers when training transformers and LSTMs for NLP, and VGG and ResNet for image classification over CIFAR10 and CIFAR100 while matching the best performance of the eight adaptive methods when training WGAN-GP models for image generation tasks. Furthermore, SET-Adam produces higher validation accuracies than Adam and AdaBelief for training ResNet18 over ImageNet.

Index Terms—Adam, adaptive optimization, DNN, transformer.

I. INTRODUCTION

In the last decade, stochastic gradient descent (SGD) and its variants have been widely applied in deep learning [1]–[4] due to their simplicity and effectiveness. In the literature, SGD with momentum [5], [6] dominates over other optimizers for image classification tasks [7], [8]. Suppose the objective function $f(\theta) : \theta \in \mathbb{R}^d$ of a DNN model is differentiable. Its update expression for minimising $f(\theta)$ can be represented as

$$\mathbf{m}_t = \beta_1 \mathbf{m}_{t-1} + \mathbf{g}_t \quad (1)$$

$$\theta_t = \theta_{t-1} - \eta_t \mathbf{m}_t, \quad (2)$$

where $\mathbf{g}_t = \nabla f(\theta_{t-1})$ is the gradient at θ_t , and η_t is the common stepsize for all the coordinates of θ .

To bring flexibility to SGD with momentum, an active research trend is to introduce elementwise adaptive stepsizes for all the coordinates of \mathbf{m}_t in (2), referred to as *adaptive optimization* [9]–[11]. In the literature, Adam [11] is probably the most popular adaptive optimization method (e.g., [2], [12]–[14]). Its update expression can be written as

$$[\text{Adam}] \begin{cases} \mathbf{m}_t = \beta_1 \mathbf{m}_{t-1} + (1 - \beta_1) \mathbf{g}_t \\ \mathbf{v}_t = \beta_2 \mathbf{v}_{t-1} + (1 - \beta_2) \mathbf{g}_t^2 \\ \theta_t = \theta_{t-1} - \eta_t \frac{1}{1 - \beta_1^t} \frac{\mathbf{m}_t}{\sqrt{\mathbf{v}_t / (1 - \beta_2^t)} + \epsilon} \end{cases}, \quad (3)$$

Algorithm 1 SET-Adam: suppressing range of adaptive stepsizes of Adam by performing three consecutive operations on $\{\mathbf{v}_t\}$

```

1: Input:  $\beta_1, \beta_2, \eta_t, \epsilon > 0, \tau = 0.5, \mathbf{1}_l = [1, 1, \dots, 1]^T$ 
2: Init.:  $\theta_0 \in \mathbb{R}^d, \mathbf{m}_0 = 0, \mathbf{v}_0 = 0 \in \mathbb{R}^d$ 
3: for  $t = 1, 2, \dots, T$  do
4:    $\mathbf{g}_t \leftarrow \nabla f(\theta_{t-1})$ 
5:    $\mathbf{m}_t \leftarrow \beta_1 \mathbf{m}_{t-1} + (1 - \beta_1) \mathbf{g}_t$ 
6:    $\mathbf{v}_t \leftarrow \beta_2 \mathbf{v}_{t-1} + (1 - \beta_2) \mathbf{g}_t^2$ 
7:   for  $l = 1, \dots, L$  do
8:      $\tilde{\mathbf{v}}_{l,t} = \mathbf{v}_{l,t} \cos^2(\angle \mathbf{v}_{l,t} \mathbf{1}_l)$  [down-scaling]
9:      $\mathbf{w}_{l,t} = \sqrt{\tilde{\mathbf{v}}_{l,t} / (1 - \beta_2^t)} + \epsilon$  [ $\epsilon$ -embedding]
10:     $\tilde{\mathbf{w}}_{l,t} = \mathbf{w}_{l,t} - \tau \left( \min_{i=1}^{d_l} \mathbf{w}_{l,t}[i] \right)$  [down-translating]
11:  end for
12:   $\tilde{\mathbf{m}}_t \leftarrow \frac{\mathbf{m}_t}{1 - \beta_1^t}$ 
13:   $\theta_t \leftarrow \theta_{t-1} - \frac{\eta_t \tilde{\mathbf{m}}_t}{\tilde{\mathbf{w}}_t}$ 
14: end for
15: Output:  $\theta_T$ 

```

where $\mathbf{g}_t = f(\theta_{t-1})$, $0 < \beta_1, \beta_2 < 1$, and $\epsilon > 0$. The two vector operations $(\cdot)^2$ and \cdot / \cdot are performed in an elementwise manner. The two exponential moving averages (EMAs) \mathbf{m}_t and \mathbf{v}_t are referred to as the first and second momentum. The two quantities $1 - \beta_1^t$ and $1 - \beta_2^t$ are introduced to compensate for the estimation bias in \mathbf{m}_t and \mathbf{v}_t , respectively. η_t is the common stepsize while $\alpha_t = 1 / (\sqrt{\mathbf{v}_t / (1 - \beta_2^t)} + \epsilon) \in \mathbb{R}^d$ represents the elementwise adaptive stepsizes.

Due to the great success of Adam in training DNNs, various extensions of Adam have been proposed, including AdamW [15], NAdam [16], Yogi [17], MSVAG [18], Fromage [19]. It is worth noting that the following three algorithms extend Adam by reducing the variance of the adaptive stepsizes in different manner. In [20], the authors suggested multiplying \mathbf{m}_t by a rectified scalar when computing θ_t in (3) when the variance is large, which is referred to as RAdam. Empirical evidence shows that RAdam produces better generalization. The AdaBound method of [21] is designed to avoid extremely large and small adaptive stepsizes of Adam, which has a similar effect as RAdam. In practice, AdaBound works as an adaptive method at the beginning of the training process and gradually transforms to SGD with momentum, where all the adaptive stepsizes tend to converge to a single value. The AdaBelief method of [22] extends Adam by tracking the EMA of the squared prediction error $(\mathbf{m}_t - \mathbf{g}_t)^2$ instead of \mathbf{g}_t^2 when

⁰Considering Adam at iteration t , the layerwise average of adaptive stepsizes for the l th layer of VGG11 is computed as $\frac{1}{d_l} \sum_{i=1}^{d_l} \alpha_{l,t}[i] = \frac{1}{d_l} \sum_{i=1}^{d_l} 1 / (\sqrt{\mathbf{v}_{l,t}[i] / (1 - \beta_2^t)} + \epsilon)$, where $\mathbf{v}_{l,t} \in \mathbb{R}^{d_l}$ is the subvector of $\mathbf{v}_t \in \mathbb{R}^d$ for the l th layer.

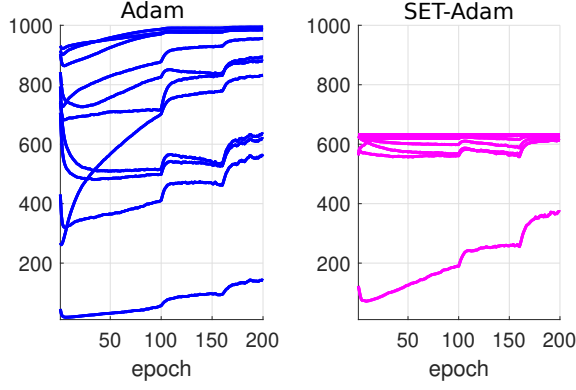


Fig. 1. Comparison of layerwise average of adaptive stepsizes for the 11 neural layers of VGG11 by training over CIFAR10 for 200 epochs. See Appendix C for the parameter setups of the two methods, where the optimal parameter ϵ for Adam was selected from a discrete set to give the best validation performance. The jumps in the curves at 100 and 160 epochs are due to the change in the common stepsize. SET-Adam has a much more compact range of layerwise average stepsizes than Adam.

computing the second momentum \mathbf{v}_t . In general, \mathbf{m}_t can be viewed as a reliable prediction of \mathbf{g}_t , making the mean and variance of $(\mathbf{m}_t - \mathbf{g}_t)^2$ across all the coordinates smaller than those of \mathbf{g}_t^2 . As a result, the variance of the adaptive stepsizes in AdaBelief would be smaller than that in Adam. Conceptually speaking, the above three methods aim to reduce the range of the adaptive stepsizes of Adam to mimic the convergence behavior of SGD with momentum to a certain extent.

Based on our observation that the gradient statistics in Adam are generally heterogeneous across different neural layers (see Fig. 1-2), we consider suppressing the range of adaptive stepsizes of Adam by using layerwise gradient statistics. Suppose at iteration t , \mathbf{v}_t is the obtained second momentum by following (3). A sequence of three operations are performed on \mathbf{v}_t (see Alg. 1 for details) before using it in the update of the DNN model θ , namely, (1): down-scaling, (2): ϵ -embedding, and (3): down-translating. The resulting algorithm is referred to as SET-Adam, where “SET” is a short notation of the three operations. Fig. 1 and 2 demonstrates that SET-Adam indeed produces a more compact range of adaptive stepsizes than Adam for training VGG11 over CIFAR10. At the end of the training process, the 11 layerwise average stepsizes in Fig. 1 do not converge to a single value, indicating the adaptability of SET-Adam.

To summarize, we make four contributions with SET-Adam.

- (a) We propose to down-scale the layerwise subvectors $\{\mathbf{v}_{l,t}\}_{l=1}^L$ of \mathbf{v}_t by exploiting the angles between the subvectors $\{\mathbf{v}_{l,t}\}_{l=1}^L$ and the corresponding all-one vectors $\{\mathbf{1}_l\}_{l=1}^L$ of the same dimensions. Specifically, the subvectors of \mathbf{v}_t of which the angles are relatively large are down-scaled to a large extent. On the other hand, a small angle indicates that the associated subvector $\mathbf{v}_{l,t}$ has roughly the same value across all its coordinates, implying this particular neural layer has great similarity to the effect of SGD with momentum at the current iteration.

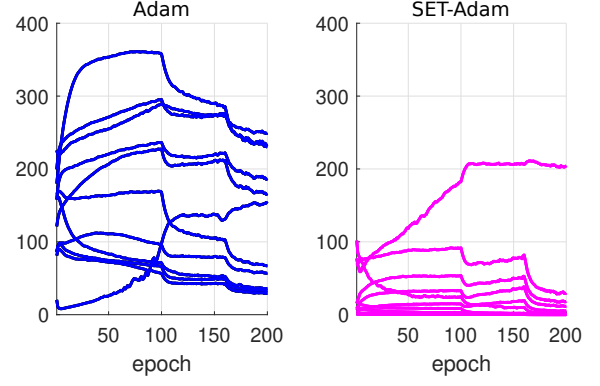


Fig. 2. Comparison of layerwise standard deviations (stds) of adaptive stepsizes for the 11 neural layers by training VGG11 over CIFAR10 for 200 epochs. SET-Adam has much smaller layerwise stds than Adam for ten out of eleven neural layers.

In this case, it is reasonable to make the down-scaling negligible. It can be shown that the above operation is able to suppress the range of adaptive stepsizes compared to Adam.

- (b) Differently from (3) of Adam, the ϵ -embedding operation puts ϵ inside the sqrt operation (see Alg. 1). We are aware that the AdaBelief optimizer also utilizes the above ϵ -embedding operation but without a proper motivation (see Appendix A for mathematical verification). We show via a Taylor expansion that putting ϵ inside the sqrt operation essentially suppresses the range of the adaptive stepsizes.
- (c) As indicated in Alg. 1, the down-translating operation subtracts a scalar value from $\mathbf{w}_{l,t}$ for the l th neural layer, where the scalar is computed as a function of $\mathbf{w}_{l,t}$. It is designed to uplift the resulting adaptive stepsizes to avoid extreme small ones, which is inspired by the design of the AdaBound optimizer. It is found that the setup $\tau = 0.5$ for controlling the strength of the down-translating works well in practice, and there is no need to tune the parameter.
- (d) Extensive experimental results show that SET-Adam yields considerably better performance than eight adaptive optimizers for training transformer [2] and LSTM [23] models in natural language processing (NLP) tasks, and VGG11 [24] and ResNet34 in image classification tasks over CIFAR10 and CIFAR100. It is also found that SET-Adam matches the best performance of the eight methods when training WGAN-GP models in image generation tasks. Lastly, SET-Adam outperforms Adam and AdaBelief when training ResNet18 on the large ImageNet dataset. The computational complexity of SET-Adam was evaluated for training VGG11 and ResNet34. The results show that SET-Adam consumes an additional 12% – 20% time per epoch compared to Adam.

Notations: We use small bold letters to denote vectors. The l_2 and l_∞ norms of a vector \mathbf{y} are denoted as $\|\mathbf{y}\|_2$ and $\|\mathbf{y}\|_\infty$, respectively. Given an L -layer DNN model θ of dimension d , we use θ_l of dimension d_l to denote the subvector of θ for the l th layer. Thus, there is $\sum_{l=1}^L d_l = d$. The i th element of θ_l is represented by $\theta_l[i]$. The notation $[L]$ stands for the set

$[L] = \{1, \dots, L\}$. Finally, the angle between two vectors \mathbf{y} and \mathbf{x} of the same dimension is denoted by $\angle \mathbf{x}\mathbf{y}$.

II. ALGORITHMIC DESIGN OF SET-ADAM

In this section, we explain in detail the three operations introduced in SET-Adam sequentially for processing the second momentum \mathbf{v}_t at iteration t (see Alg. 1). We point out that the first two operations *down-scaling* and ϵ -*embedding* suppress the range of adaptive stepsizes of Adam while the last operation *down-translating* uplifts the resulting adaptive stepsizes to avoid extreme small ones. A convex convergence analysis for SET-Adam is presented at the end of the section.

A. Motivation of layerwise down-scaling operation

Motivated by the existing work [20]–[22], we would like to reduce the range of the adaptive stepsizes of Adam to make the new optimizer get closer to SGD with momentum. To achieve the above goal, we consider processing the second momentum \mathbf{v}_t of (3) in a layerwise manner before using it to update a DNN model $\boldsymbol{\theta}$. In general, the parameters within the same neural layer are functionally homogeneous when processing data from the layer below. It is likely that the gradients within the same layer follow a single distribution, making it natural to perform layerwise processing. On the other hand, the gradient statistics can be quite different across different neural layers due to progressive nonlinear processing from bottom to top layers. See Fig. 1-2 for the heterogeneous layerwise curves of Adam. Finally, it is computationally more efficient to perform layerwise processing than operating on the entire vector \mathbf{v}_t due to the nature of back-propagation when training the model $\boldsymbol{\theta}$.

We now consider what kind of layerwise processing would be desirable to extend Adam. Firstly, we note that the parameter ϵ of (3) in Adam defines an upper bound on the adaptive stepsizes and is independent of neural layer and iteration indices. We use $\mathbf{v}_{l,t}$ and $\boldsymbol{\alpha}_{l,t}$ to denote the subvectors of \mathbf{v}_t and $\boldsymbol{\alpha}_t$ for the l th neural layer, respectively. It is immediate that the upper bound¹ is

$$\frac{1}{\epsilon} \geq \max_{l=1}^L \max_{i=1}^{d_l} \left(\alpha_{l,t}[i] = 1 / \left(\sqrt{\mathbf{v}_{l,t}[i] / (1 - \beta_2^t)} + \epsilon \right) \right). \quad (4)$$

Suppose we replace each $\mathbf{v}_{l,t}$ in (4) by $\gamma_{l,t} \mathbf{v}_{l,t}$, where $\gamma_{l,t} \in (0, 1)$. If the scalars $\{\gamma_{l,t}\}_{l=1}^L$ are sufficiently small in the extreme case, all the adaptive stepsizes of the new method tend to approach the upper bound in (4). As a result, the new method will have a smaller range of adaptive stepsizes than Adam either in a layerwise manner or globally.

We propose to compute the scalar $\gamma_{l,t}$ for $\mathbf{v}_{l,t}$ as a function of the angle $\angle \mathbf{v}_{l,t} \mathbf{1}_l$ between the subvector $\mathbf{v}_{l,t}$ and the corresponding all-one vector $\mathbf{1}_l = [1, 1, \dots, 1]^T$. The angles $\{\angle \mathbf{v}_{l,t} \mathbf{1}_l\}_{l=1}^L$ reflect the variances of $\{\mathbf{v}_{l,t}\}_{l=1}^L$ across their respective coordinates to a certain extent, which are different across different layers. By doing so, we implicitly take into account the heterogeneity of layerwise gradient statistics instead

$\mathbf{v}_{l,t}$: 2nd momentum for the l th layer

$\mathbf{1}_l = [1, 1, \dots, 1]^T$

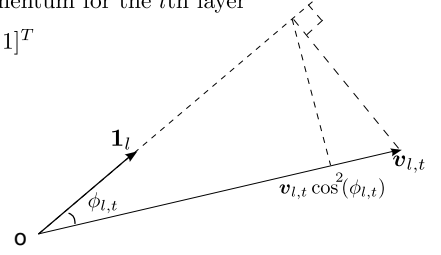


Fig. 3. Demonstration of the *down-scaling* operation in SET-Adam. The vector $\mathbf{1}_l$ is of the same dimension as $\mathbf{v}_{l,t}$.

of setting an iteration-dependent common value for $\gamma_{l,t}$ across all neural layers.

On the other hand, RAdam and AdaBound in the literature do not take into account the heterogeneity of statistics in $\{\mathbf{v}_{l,t}\}_{l=1}^L$ across different layers. This might be the reason that the empirical performance of SET-Adam is better than the above two optimizers as will be demonstrated in Section III.

B. Design of layerwise down-scaling operation

Consider the l th layer of a DNN model at iteration t . We down-scale $\mathbf{v}_{l,t}$ by a scalar $\gamma_{l,t}$, given by²

$$\tilde{\mathbf{v}}_{l,t} = \gamma_{l,t} \mathbf{v}_{l,t} = \cos^2(\angle \mathbf{v}_{l,t} \mathbf{1}_l) \mathbf{v}_{l,t} \quad (5)$$

As illustrated in Fig. 3, the quantity $\tilde{\mathbf{v}}_{l,t}$ can be viewed as performing two vector projections between $\mathbf{v}_{l,t}$ and $\mathbf{1}_l$. That is, we first project $\mathbf{v}_{l,t}$ onto the vector direction $\mathbf{1}_l / \|\mathbf{1}_l\|$, and then project back the obtained vector onto the vector direction $\mathbf{v}_{l,t} / \|\mathbf{v}_{l,t}\|$.

Our motivation for choosing the all-one vector $\mathbf{1}_l$ as a reference for the angle computation is that we would like to push the adaptive stepsizes of Adam to be much more compact so that the new optimizer has a similar effect as that of SGD with momentum. With the expression (5), it is natural that those layerwise subvectors of \mathbf{v}_t with large angles $\{\angle \mathbf{v}_{l,t} \mathbf{1}_l\}$ are down-scaled to a large extent. On the contrary, a small angle implies that all the elements in the associated subvector $\mathbf{v}_{l,t}$ are roughly the same. In this case, the scalar $\gamma_{l,t}$ is close to 1, suggesting that the down-scaling operation is negligible as desired.

For the extreme case that each neural layer has only one parameter (i.e., $\mathbf{v}_{l,t} \in \mathbb{R}, \forall l \in [L]$), it is immediate that $\gamma_{l,t} = \cos^2(\angle \mathbf{v}_{l,t} \mathbf{1}_l) = 1$. That is, the down-scaling operation has no effect, which is safe from the viewpoint of implementation stability.

C. ϵ -embedding for suppressing range of adaptive stepsizes

It is known from literature that the ϵ parameter is originally introduced in adaptive optimizers to avoid division by zero. In this subsection, we show that the placement of the ϵ parameter in the update expressions has a significant impact on the adaptive stepsizes. In particular, we will show in the following that by a Taylor approximation that putting the ϵ parameter

¹For the case that ϵ is inside the sqrt operation, the upper bound becomes $\frac{1}{\sqrt{\epsilon}} \geq \max_{l=1}^L \max_{i=1}^{d_l} (\alpha_{l,t}[i] = 1 / \sqrt{\mathbf{v}_{l,t}[i] / (1 - \beta_2^t)} + \epsilon)$. In this case, the motivation for down-scaling still holds.

²We have also considered the high-order case $\gamma_{l,t} = \cos^n(\angle \mathbf{v}_{l,t} \mathbf{1}_l)$, $n = 4$. It is empirically found that $n = 4$ makes the down-scaling operation too aggressive while at the same time incurring additional computation cost. We therefore ignore the high-order cases in the main paper.

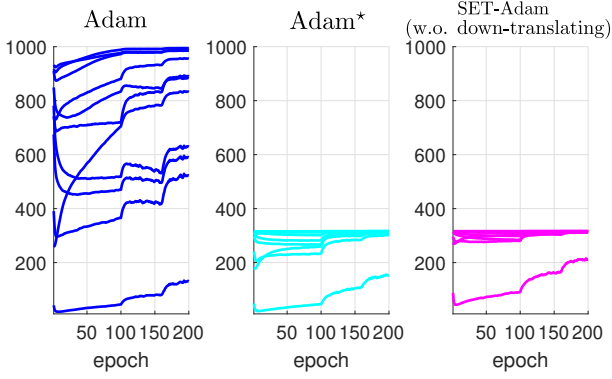


Fig. 4. Comparison of layerwise average of adaptive stepsizes for the 11 neural layers by training VGG11 over CIFAR10 for 200 epochs. For the plot of SET-Adam, the down-translating operation is ignored and only the first two operations are included. See Appendix C for the algorithmic parameter setups.

inside the sqrt operation of (3) in Adam helps to suppress the range of adaptive stepsizes.

Suppose Adam* is obtained by putting ϵ inside the sqrt operation in (3) (see Appendix B for Adam*). We now study the modified adaptive stepsizes in Adam*: $\tilde{\alpha}_t = 1/\sqrt{v_t/(1-\beta_2^t) + \epsilon}$, which can be approximated to be

$$\tilde{\alpha}_t = 1/\sqrt{v_t/(1-\beta_2^t) + \epsilon} \quad (6)$$

$$\approx \underbrace{\frac{1}{\sqrt{v_t/(1-\beta_2^t)}}}_{\text{1st term}} + \underbrace{\frac{1}{2\sqrt{v_t/(1-\beta_2^t)}}\epsilon}_{\text{2nd term}}, \quad (7)$$

where the Taylor approximation is applied to a function $h(x) = \sqrt{a+x}$ around $x=0$, where $x=\epsilon$ and $a=v_t/(1-\beta_2^t)$.

Next we investigate (7). Generally speaking, small elements of v_t lead to large adaptive stepsizes while large elements lead to small adaptive stepsizes due to the inverse operation $1/(\cdot)$. It is clear from (7) that for small elements of v_t , the second term in the denominator is relatively large, implicitly penalizing large stepsizes. Furthermore, (6) indicates that those large stepsizes are upper-bounded by the quantity $1/\sqrt{\epsilon}$. In contrast, for large elements of v_t , the second term is relatively small, thus reducing the occurrence of extremely small adaptive stepsizes. In short, moving ϵ from outside of the sqrt operation to inside helps to suppress the range of adaptive stepsizes in Adam.

Similarly, employment of the ϵ -embedding in SET-Adam would also help to suppress the range of adaptive stepsizes. Mathematically, applying the ϵ -embedding on $\tilde{w}_{l,t}$ of (5) leads to

$$\begin{aligned} w_{l,t} &= \sqrt{\tilde{v}_{l,t}/(1-\beta_2^t) + \epsilon} \\ &= \sqrt{\cos^2(\angle v_{l,t} \mathbf{1}_l) v_{l,t}/(1-\beta_2^t) + \epsilon}. \end{aligned} \quad (8)$$

As we mentioned earlier, AdaBelief also utilizes ϵ -embedding in the update expressions (see Appendix A for verification), which might be another reason AdaBelief outperforms Adam.

Fig. 4 demonstrates that Adam* indeed has a more compact range of adaptive stepsizes than Adam due to the proper placement of the ϵ parameter. SET-Adam without the down-translating operation further suppresses the range of adaptive stepsizes of Adam* due to the additional down-scaling operation. At epoch 200, the eleven layerwise average stepsizes in Adam are distributed in $[190, 1000]$ while ten out of eleven layerwise average stepsizes in SET-Adam are close to a single value of 320.

D. Down-translating for avoiding extreme small adaptive stepsizes

We notice that due to the ϵ -embedding operation in (8), the elements in the subvector $w_{l,t}$ are lower-bounded by the positive scalar $\sqrt{\epsilon}$, i.e., $w_{l,t}[i] \geq \sqrt{\epsilon}, \forall i$. We propose to further subtract a scalar from $w_{l,t}$ to avoid extreme small adaptive stepsizes in SET-Adam, which is given by

$$\tilde{w}_{l,t} = w_{l,t} - \tau \left(\min_{i=1}^{d_l} w_{l,t}[i] \right), \quad (9)$$

where $0 \leq \tau < 1$ is imposed to ensure that all the elements of $\tilde{w}_{l,t}$ are positive. It is not difficult to show that

$$(1-\tau)\sqrt{\epsilon} \leq \tilde{w}_{l,t}[i] \quad \forall i = 1, \dots, d_l. \quad (10)$$

That is, the subvector $\tilde{w}_{l,t}$ is lower-bounded by $(1-\tau)\sqrt{\epsilon}$. Once all the subvectors $\{\tilde{w}_{l,t}\}_{l=1}^L$ are obtained from (9), the DNN model θ can be updated in the form of

$$\theta^t = \theta^{t-1} - \eta \tilde{m}_t / \tilde{w}_t,$$

where the adaptive stepsizes are $\alpha_t = 1/\tilde{w}_t$.

By inspection of the behaviors of SET-Adam in Figs. 1 and 4, it can be seen that the down-translating operation manages to uplift the resulting adaptive stepsizes of SET-Adam in Fig. 1, which implicitly avoids extreme small adaptive stepsizes as expected.

E. Convergence analysis

In this paper, we focus on convex optimization for SET-Adam. Our analysis follows a strategy similar to that used to analyze AdaBelief in [22].

Theorem 1. Suppose $\{\theta_t\}_{t=0}^T$ and $\{\tilde{w}_t\}_{t=0}^T$ are the iterative updates obtained by running SET-Adam³ starting with $(m_0, v_0) = (\mathbf{0}, \mathbf{0})$. Let $0 \leq \beta_{1t} = \beta_1 \lambda^t < 1, 0 \leq \beta_2 < 1$, and $\eta_t = \frac{\eta}{\sqrt{t}}$. Assume (1): $f(\theta)$ is a differentiable convex function with $\|g_t\|_\infty \leq G_\infty \sqrt{1-\beta_2}$ for all $t \in [T]$; (2): the updates $\{\theta_t\}_{t=0}^T$ and the optimal solution θ^* are bounded by a hyper-sphere, i.e., $\|\theta_t\|_2 \leq D$ and $\|\theta^*\|_2 \leq D$; (3): $0 < \sqrt{c} \leq \tilde{w}_t[i] \leq \tilde{w}_{t-1}[i]$ for all $i \in \{1, \dots, d\}$ and $t \in [T]$. Denote $\bar{\theta}_T = \frac{1}{T} \sum_{t=0}^{T-1} \theta_t$ and $\mathbf{g}_{1:T}^2[i] = ((g_1[i])^2, \dots, (g_T[i])^2) \in \mathbb{R}^T$. We then have the following bound on regret:

$$\begin{aligned} f(\bar{\theta}_T) - f(\theta^*) &\leq \frac{2D^2 d(G_\infty + \sqrt{\epsilon})}{\eta(1-\beta_1)T} + \frac{2D^2 d(G_\infty + \sqrt{\epsilon})}{\sqrt{T}(1-\beta_1)\eta} \\ &\quad + \frac{(1+\beta_1)\eta\sqrt{1+\log T}}{2\sqrt{c}(1-\beta_1)^3 T} \sum_{i=1}^d \|\mathbf{g}_{1:T}^2[i]\|_2 + \frac{2D^2 d\beta_1(G_\infty + \sqrt{\epsilon})}{(1-\beta_1)(1-\lambda)^2 \eta T}. \end{aligned} \quad (11)$$

³ β_1 in Algorithm 1 is generalized to be $\beta_{1t}, t \geq 0$ to facilitate convergence analysis. AdaBelief was analyzed in a similar manner.

Proof. see Appendix D for the proof. \square

Remark 1. The condition $0 < \sqrt{c} \leq \tilde{w}_t[i]$ in Theorem 1 follows directly from (10). The assumptions $\tilde{w}_t[i] \leq \tilde{w}_{t-1}[i]$ for all (i, t) are also reasonable as t increases, the gradient-magnitudes tend to approach to zero.

III. EXPERIMENTS

We evaluated SET-Adam on three types of DNN tasks: (1) natural language processing (NLP) on training transformer and LSTM models; (2) image classification on training VGG and ResNet [7] models; (3) image generation on training WGAN-GP [25]. Two open-source repositories⁴ were used for the above DNN training tasks. To demonstrate the effectiveness of the proposed method, eight adaptive optimizers from the literature were tested and compared, namely Yogi [17], RAdam [20], MSVAG [18], Fromage [19], Adam [11], AdaBound [21], AdamW [15], and AdaBelief [22]. In addition, SGD with momentum was evaluated as a baseline for performance comparison. In all experiments, the additional parameter τ in SET-Adam was set to $\tau = 0.5$, and not tuned for each DNN task for simplicity.

It is found that SET-Adam outperforms the eight adaptive optimizers for training transformer, LSTM, VGG11, and ResNet34 models while it matches the best performance of the eight methods for training WGAN-GP. The non-adaptive method SGD with momentum produce good performance only when training VGG11 and ResNet34. Lastly, experiments on training ResNet18 on the large ImageNet dataset show that SET-Adam outperforms Adam and AdaBelief.

The time complexity of SET-Adam was evaluated for training VGG11 and ResNet34 on a 2080 Ti GPU. In brief, SET-Adam consumed 12% – 20% more time per epoch compared to Adam.

A. On training a transformer

In this task, we consider the training of a transformer for WMT16: multimodal translation by using the first open-source as indicated in the footnote. In the training process, we retained almost all of the default hyper-parameters provided in the open-source except for the batch size. Due to limited GPU memory, we changed the batch size from 256 to 200. The parameters of SET-Adam were set to $(\eta_0, \beta_1, \beta_2, \epsilon, \tau) = (0.001, 0.9, 0.98, 1e-15, 0.5)$. The parameter-setups for other optimizers can be found in Table VII of Appendix E, where certain hyper-parameters for each optimizer were searched over some discrete sets to optimize the validation performance. For example, the parameter ϵ of Adam was searched over the set $\{1e-6, 1e-7, \dots, 1e-12\}$ while the remaining parameters were set to $(\eta_0, \beta_1, \beta_2) = (0.001, 0.9, 0.98)$ as in SET-Adam. Once the optimal parameter-configuration for each optimizer

⁴<https://github.com/jadore801120/attention-is-all-you-need-pytorch> is adopted for the task of training a transformer, which produces reasonable validation performance using Adam. <https://github.com/juntang-zhuang/Adabelief-Optimizer> is adopted for all the remaining tasks. The second open source is the original implementation of AdaBelief [22].

TABLE I
PERFORMANCE COMPARISON FOR TRAINING THE TRANSFORMER.

SGD (non-adaptive)	55.58±0.34	AdaBound	55.90±0.21
Yogi	60.47±0.61	RAdam	64.47±0.19
MSVAG	53.79±0.13	Fromage	55.57±0.19
AdamW	64.49±0.24	AdaBelief	66.90±0.77
Adam	64.71±0.57	SET-Adam (Our)	69.19±0.09

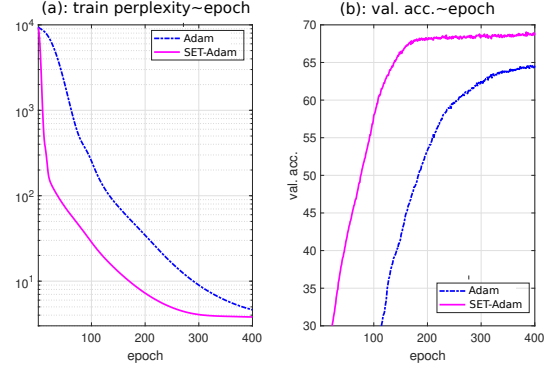


Fig. 5. Performance visualisation of Adam and SET-Adam for the training of the transformer.

was obtained by searching, three experimental repetitions were then performed to alleviate the effect of the randomness.

It is clear from Table I that SET-Adam significantly outperforms all other methods. We emphasize that the maximum number of epochs was set to 400 for each optimizer by following the default setup in the open source, and no epoch cutoff is performed in favor of SET-Adam. Fig. 5 demonstrates that SET-Adam not only converges faster in the training process than Adam but also produces much better validation accuracy. On the other hand, the non-adaptive method SGD with momentum produces a performance that is inferior to all adaptive methods except Fromage and MSVAG.

B. On training LSTMs

In this experiment, we consider training LSTMs with a different number of layers over the Penn TreeBank dataset [26]. The detailed experimental setup such as dropout rate and gradient-clipping magnitude can be found in the first open-source repository provided in the footnote. Similar to the task of training the transformer, the optimizers have both fixed and free parameters of which the free parameters remain to be searched over some discrete sets. See Table VIII in Appendix E for a summary of the fixed and free parameters for each optimizer. An example is Adam for which $\eta_0 \in \{0.01, 0.001\}$ and $\epsilon \in \{1e-6, 1e-8, 1e-10, 1e-12\}$ were tested to find the optimal configuration that produces the best validation performance.

Table. II summarises the obtained validation perplexities of the ten methods for training 1, 2, and 3-layer LSTMs. It was found that for each optimizer, independent experimental repetitions lead to almost the same validation perplexity value. Therefore, we only keep the average of the validation perplexity values from three independent experimental repetitions for

TABLE II
VALIDATION PERPLEXITY ON PENN TREEBANK FOR 1, 2, 3-LAYER LSTM. **LOWER IS BETTER.**

	SGD (non-adaptive)	AdaBelief	AdamW	Yogi	AdaBound
1 layer	85.52	84.21	88.36	86.78	84.52
2 layer	67.44	66.29	73.18	71.56	67.01
3 layer	63.68	61.23	70.08	67.83	63.16
	SET-Adam	Adam	RAadam	MSVAG	Fromage
1 layer	78.54	84.28	88.76	84.75	85.20
2 layer	64.80	66.86	74.12	68.91	72.22
3 layer	60.86	64.28	70.41	65.04	67.37

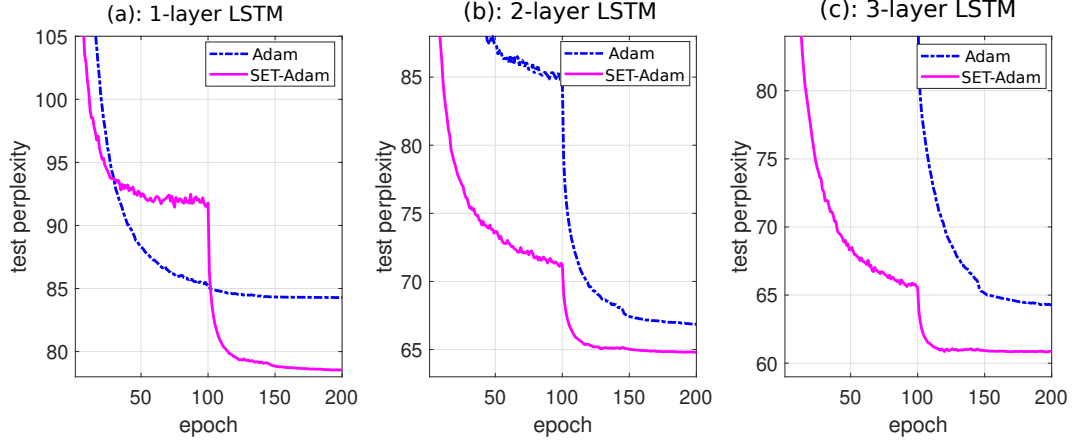


Fig. 6. Performance visualisation of SET-Adam and Adam in Table II.

TABLE III
VALIDATION ACCURACIES (IN PERCENTAGE) AND **TIME COMPLEXITY IN SECONDS PER EPOCH (REFERRED TO AS *t. c.*)** OF TEN METHODS FOR TRAINING VGG11 AND RESNET34 OVER CIFAR10 AND CIFAR100. THE BEST RESULT IS HIGHLIGHTED IN EACH COLUMN.

	CIFAR10				CIFAR100			
	VGG11		ResNet34		VGG11		ResNet34	
optimizers	val. acc	t. c.	val. acc	t. c.	val. acc	t. c.	val. acc	t. c.
SGD (non-adaptive)	91.36 \pm 0.07	5.83	95.48 \pm 0.11	30.45	67.02 \pm 0.25	5.85	78.10 \pm 0.18	30.92
Yogi	90.74 \pm 0.16	6.49	94.98 \pm 0.26	31.74	65.57 \pm 0.17	6.42	77.17 \pm 0.12	32.20
RAadam	89.58 \pm 0.10	6.28	94.64 \pm 0.18	31.21	63.62 \pm 0.20	6.29	74.87 \pm 0.13	31.58
MSVAG	90.04 \pm 0.22	7.08	94.65 \pm 0.08	33.78	62.67 \pm 0.33	7.19	75.57 \pm 0.14	33.80
Fromage	89.72 \pm 0.25	6.66	94.64 \pm 0.07	35.19	62.93 \pm 0.53	6.56	74.84 \pm 0.27	35.50
AdamW	89.46 \pm 0.08	6.25	94.48 \pm 0.18	31.71	62.50 \pm 0.23	6.31	74.29 \pm 0.20	31.80
AdaBound	90.48 \pm 0.12	6.71	94.73 \pm 0.16	33.75	64.80 \pm 0.42	6.73	76.15 \pm 0.10	33.78
AdaBelief	91.55 \pm 0.13	6.47	95.15 \pm 0.11	31.66	68.05 \pm 0.31	6.49	77.32 \pm 0.37	31.74
Adam	91.20 \pm 0.21	6.15	95.09 \pm 0.18	31.28	67.88 \pm 0.13	6.20	77.31 \pm 0.14	31.47
SET-Adam (our)	91.89\pm0.17	7.40	95.47 \pm 0.06	36.25	69.93\pm0.20	7.21	77.75 \pm 0.45	35.10

TABLE IV
BEST FID OBTAINED FOR EACH OPTIMIZER (**LOWER IS BETTER**)

	Adam	AdaBelief	AdamW	RAadam	AdaBound
best FIDs	66.71	56.73	63.76	69.14	61.65
	SET-Adam	MSVAG	SGD	Yogi	Fromage
best FIDs	57.42	69.47	90.61	68.34	78.47

each experimental setup in the table and ignore the standard deviations.

It is clear from Table. II that SET-Adam again outperforms all other methods in all three scenarios, which may be due to the contribution of a compact range of adaptive stepsizes in SET-Adam. Fig. 6 further visualised the validation performance of SET-Adam compared to Adam. The performance gain of SET-Adam is considerable in all three scenarios.

C. On training VGG11 and ResNet34 over CIFAR10 and CIFAR100

In this task, the ten optimizers were evaluated by following a similar experimental setup as in [22]. The batch size and epoch were set to 128 and 200, respectively. The common stepsize η_t is reduced by multiplying by 0.1 at 100 and 160 epoch. The detailed parameter-setups for the optimizers can be found in Table X in Appendix E. Three experimental repetitions

TABLE V
VALIDATION ACCURACIES (IN PERCENTAGE) OF THE OPTIMIZERS
FOR TRAINING RESNET18 OVER IMAGENET.

optimizers	AdaBelief	Adam	SET-Adam
val. acc.	69.65	69.03	69.77

were conducted for each optimizer to alleviate the effect of randomness.

Both the validation performance and the algorithmic complexity are summarised in Table III. It is clear that SET-Adam consistently outperforms the eight *adaptive* optimizers in terms of validation accuracies. This demonstrates that the compact range of adaptive stepsizes in SET-Adam does indeed improve the generalization performance. The non-adaptive optimizer SGD with momentum demonstrates good performance, confirming the findings in [7], [8] that this optimizer dominates over adaptive optimizers in image classification tasks.

We can also conclude from the table that SGD with momentum is the most computationally efficient method. On the other hand, due to the three operations, SET-Adam consumed an additional 12% – 20% time per epoch compared to Adam.

D. On training WGAN-GP over CIFAR10

This task focuses on training WGAN-GP. The parameters of SET-Adam were set to $(\eta_t, \beta_1, \beta_2, \epsilon, \tau) = (0.0002, 0.5, 0.999, 1e-11, 0.5)$. The parameter-setups of other optimizers can be found in Table IX of Appendix E. As an example, the parameter ϵ of Adam is searched over the discrete set $\{1e-4, 1e-6, \dots, 1e-14\}$. For each parameter-configuration of an optimizer, three experimental repetitions were performed due to the relatively unstable Frechet inception distance (FID) scores in training WGAN-GP.

Table IV shows the best FID for each method. Considering Adam for example, it has six parameter-configuration due to six ϵ values being tested. As a result, the best FID for Adam is obtained over 18 values, accounting for three experimental repetitions for each of six ϵ values. It can be seen from the table that SET-Adam provides comparable performance to AdaBelief, while the other methods including Adam perform significantly worse.

E. On training ResNet18 over ImageNet

In the last experiment, we investigated the performance gain of SET-Adam compared to Adam and AdaBelief for training ResNet18 on the large ImageNet dataset. The maximum epoch and minibatch size were set to 90 and 256, respectively. The common stepsize η_t is dropped by a factor of 0.1 at 70 and 80 epochs. The parameter setup for the three optimizers can be found in Table VI of Appendix E.

It is clear from Table V that for the large ImageNet dataset, SET-Adam again performs better than Adam and AdaBelief, indicating that the performance gain of SET-Adam is robust against different sizes of datasets.

Fig. 7 visualizes the training and validation curves of Adam and SET-Adam. Interestingly, it is seen that Adam exhibits better training accuracy and worse validation accuracy than SET-Adam. The above results are consistent with the findings in [8]. In particular, in [8], the authors empirically found

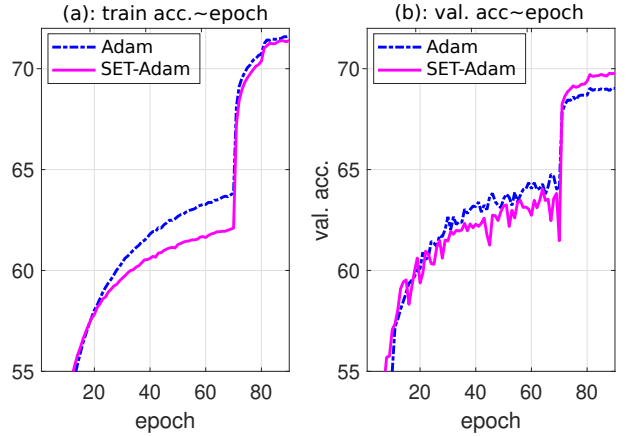


Fig. 7. Performance visualisation of Adam and SET-Adam for the training of ResNet18 over ImageNet.

that Adam performs better than SGD with momentum in the training process while producing worse validation performance in different DNN tasks. The validation performance gain of SET-Adam in Fig. 7 can be explained by the property that SET-Adam is designed to be closer to SGD with momentum.

IV. CONCLUSIONS

In this paper, we have shown that the range of the adaptive stepsizes of DNN optimizers has a significant impact on performance. The proposed SET-Adam optimizer suppresses the range of the adaptive stepsizes of Adam making it closer to SGD with momentum. Our experimental results indicate that SET-Adam will be able to produce better performance across a wide range of DNN-based applications.

In the design of the SET-Adam optimizer, we have proposed to perform a sequence of three operations on the second momentum v_t at iteration t for the purpose of reducing the range of adaptive stepsizes in Adam while avoiding extreme small ones. We realize the down-scaling operation in SET-Adam by exploiting the angles between the layerwise subvectors $\{v_{i,t}\}_{i=1}^L$ of v_t and the corresponding all-one vectors $\{1_i\}_{i=1}^L$.

Our empirical study shows that SET-Adam outperforms eight *adaptive* optimizers including Adam and AdaBelief for training transformer, LSTM, VGG11, and ResNet34 models while at the same time it matches the best performance of the eight adaptive methods for training WGAN-GP models. In addition, experiments on training ResNet18 over the large ImageNet dataset show that SET-Adam performs better than Adam and AdaBelief. On the other hand, it was found that SGD with momentum only produces good performance in image classification tasks. This suggests that the *adaptivity* of SET-Adam is important, allowing the method to effectively train different types of DNN models.

REFERENCES

- [1] Y. LeCun, Y. Bengio, and G. Hinton, “Deep Learning,” *Nature*, vol. 521, pp. 436–444, 2015.
- [2] A. Vaswani, N. Shazeer, N. Parmar, J. Uszkoreit, L. Jones, A. N. Gomez, L. Kaiser, and I. Polosukhin, “Attention is all you need,” arXiv:1706.03762 [cs. CL], 2017.
- [3] D. S. et al., “Mastering the game of Go with deep neural networks and tree search,” *Nature*, vol. 529, no. 7587, pp. 484–489, 2016.

- [4] N. Chen, Y. Zhang, H. Zen, R. J. Weiss, M. Norouzi, and W. Chan, “WaveGrad: Estimating Gradients for Waveform Generation,” arXiv:2009.00713, September 2020.
- [5] H. Sutskever, J. Martens, G. Dahl, and G. Hinton, “On the importance of initialization and momentum in deep learning,” in *International conference on Machine Learning (ICML)*, 2013.
- [6] B. T. Polyak, “Some methods of speeding up the convergence of iteration methods,” *USSR Computational Mathematics and Mathematical Physics*, vol. 4, pp. 1–17, 1964.
- [7] K. He, X. Zhang, S. Ren, and J. Sun, “Deep Residual Learning for Image Recognition,” in *IEEE conference on Computer Vision and Pattern Recognition (CVPR)*, 2015.
- [8] A. C. Wilson, R. Roelofs, M. Stern, N. Srebro, and B. Recht, “The Marginal Value of Adaptive Gradient Methods in Machine Learning,” in *31st Conference on Neural Information Processing Systems (NIPS)*, 2017.
- [9] J. Duchi, E. Hazan, and Y. Singer, “Adaptive Subgradient Methods for Online Learning and Stochastic Optimization,” *Journal of Machine Learning Research*, vol. 12, pp. 2121–2159, 2011.
- [10] T. Tieleman and G. Hinton, “Lecture 6.5-RMSProp: Divide The Gradient by a Running Average of Its Recent Magnitude,” COURSE: Neural networks for machine learning, pp. 26–31, 2012.
- [11] D. P. Kingma and J. L. Ba, “Adam: A Method for Stochastic Optimization,” arXiv preprint arXiv:1412.6980v9, 2017.
- [12] Z. Liu, Y. Lin, Y. Cao, H. Hu, Y. Wei, Z. Zhang, S. Lin, and B. Guo, “Swin Transformer: Hierarchical Vision Transformer using Shifted Windows,” in *International Conference on Computer Vision (ICCV)*, 2021.
- [13] J. Zhang, S. P. Karimireddy, A. Veit, S. Kim, S. J. Reddi, S. Kumar, and S. Sra, “Why ADAM Beats SGD for Attention Models,” in *submitted for review by ICLR*, 2019.
- [14] K. L. J. Devlin, M.-W. Chang and K. Toutanova, “Bert: Pre-training of deep bidirectional transformers for language understanding,” arXiv:1810.04805, 2018.
- [15] I. Loshchilov and F. Hutter, “Decoupled Weight Decay Regularization,” in *ICLR*, 2019.
- [16] T. Dozat, “Incorporating Nesterov Momentum into Adam,” in *International conference on Learning Representations (ICLR)*, 2016.
- [17] M. Zaheer, S. Reddi, D. Sachan, S. Kale, and S. Kumar, “Adaptive methods for nonconvex optimization,” in *Advances in neural information processing systems (NeurIPS)*, 2018, p. 9793–9803.
- [18] L. Balles and P. Hennig, “Dissecting adam: The sign, magnitude and variance of stochastic gradients,” arXiv preprint arXiv:1705.07774, 2017.
- [19] J. Bernstein, A. Vahdat, Y. Yue, and M.-Y. Liu, “On the distance between two neural networks and the stability of learning,” arXiv preprint arXiv:2002.03432, 2020.
- [20] L. Liu, H. Jiang, P. He, W. Chen, X. Liu, J. Gao, and J. Han, “On the variance of the adaptive learning rate and beyond,” arXiv preprint arXiv:1908.03265, 2019.
- [21] L. Luo, Y. Xiong, Y. Liu, and X. sun, “Adaptive Gradient Methods with Dynamic Bound of Learning Rate,” in *ICLR*, 2019.
- [22] J. Zhuang, T. Tang, S. T. Y. Ding, N. Dvornek, X. Papademetris, and J. S. Duncan, “AdaBelief Optimizer: Adapting Stepsizes by the Belief in Observed Gradients,” in *NeurIPS*, 2020.
- [23] S. Hochreiter and J. Schmidhuber, “Long Short-Term Memory,” *Neural Computation*, vol. 9, no. 8, pp. 1735–1780, 1997.
- [24] K. Simonyan and A. Zisserman, “Very deep convolutional networks for large-scale image recognition,” arXiv preprint arXiv:1409.1556, 2014.
- [25] I. Gulrajani, F. Ahmed, M. Arjovsky, V. Dumoulin, and A. C. Courville, “Improved training of wasserstein gans,” in *Advances in neural information processing systems*, 2017, pp. 5767–5777.
- [26] M. Marcus, B. Santorini, and M. A. Marcinkiewicz, “Building a large annotated corpus of english: The penn treebank,” 1993. [Online]. Available: <https://catalog.ldc.upenn.edu/docs/LDC95T7/c193.html>

APPENDIX A
VERIFICATION THAT ADABELIEF ALSO UTILIZES THE ϵ -EMBEDDING OPERATION

The update expressions of AdaBelief are given by [22]

$$[\text{AdaBelief}] \begin{cases} \mathbf{m}_t = \beta_1 \mathbf{m}_{t-1} + (1 - \beta_1) \mathbf{g}_t \\ \mathbf{s}_t = \beta_2 \mathbf{s}_{t-1} + (1 - \beta_2) (\mathbf{m}_t - \mathbf{g}_t)^2 + \epsilon, \\ \boldsymbol{\theta}_t = \boldsymbol{\theta}_{t-1} - \eta_t \frac{1}{1 - \beta_1^t} \frac{\mathbf{m}_t}{\sqrt{\mathbf{s}_t / (1 - \beta_2^t) + \epsilon}} \end{cases}, \quad (12)$$

where the parameter ϵ is involved in the computation of both \mathbf{s}_t and $\boldsymbol{\theta}_t$ in AdaBelief, which is different from that of Adam. The second ϵ for computing $\boldsymbol{\theta}_t$ can be ignored in (12) since the first ϵ dominates the second one.

By simple algebra, one can show that (12) can be reformulated to be

$$[\text{AdaBelief}] \begin{cases} \mathbf{m}_t = \beta_1 \mathbf{m}_{t-1} + (1 - \beta_1) \mathbf{g}_t \\ \mathbf{s}_t = \beta_2 \mathbf{s}_{t-1} + (1 - \beta_2) (\mathbf{m}_t - \mathbf{g}_t)^2 \\ \boldsymbol{\theta}_t = \boldsymbol{\theta}_{t-1} - \eta_t \frac{1}{1 - \beta_1^t} \frac{\mathbf{m}_t}{\sqrt{\mathbf{s}_t / (1 - \beta_2^t) + \epsilon / (1 - \beta_2)}} \end{cases}, \quad (13)$$

where the second ϵ is ignored. The above expression shows that AdaBelief indeed utilizes the ϵ -embedding operation as we do.

APPENDIX B
UPDATE PROCEDURE OF ADAM*

The parameter ϵ is put inside of the sqrt $\sqrt{\cdot}$ operation to verify if Adam* has a small range of adaptive stepsizes than Adam.

Algorithm 2 Adam*

```

1: Input:  $\beta_1, \beta_2, \eta_t, \epsilon > 0$ 
2: Init.:  $\boldsymbol{\theta}_0 \in \mathbb{R}^d, \mathbf{m}_0 = 0, \mathbf{v}_0 = 0 \in \mathbb{R}^d$ 
3: for  $t = 1, 2, \dots, T$  do
4:    $\mathbf{g}_t \leftarrow \nabla f(\boldsymbol{\theta}_{t-1})$ 
5:    $\mathbf{m}_t \leftarrow \beta_1 \mathbf{m}_{t-1} + (1 - \beta_1) \mathbf{g}_t$ 
6:    $\mathbf{v}_t \leftarrow \beta_2 \mathbf{v}_{t-1} + (1 - \beta_2) \mathbf{g}_t^2$ 
7:    $\tilde{\mathbf{m}}_t \leftarrow \frac{\mathbf{m}_t}{1 - \beta_1^t} \quad \tilde{\mathbf{v}}_t \leftarrow \frac{\mathbf{v}_t}{1 - \beta_2^t}$ 
8:    $\boldsymbol{\theta}_t \leftarrow \boldsymbol{\theta}_{t-1} - \frac{\eta_t}{\sqrt{\tilde{\mathbf{v}}_t + \epsilon}} \tilde{\mathbf{m}}_t$ 
9: end for
10: Output:  $\boldsymbol{\theta}_T$ 

```

APPENDIX C
PARAMETER SETUPS FOR OPTIMIZATION METHODS IN FIG. 1-2 AND FIG. 4

The common stepsize η_t is dropped by a factor 0.1 at 100 and 160 epochs. The optimal parameter ϵ is searched over the set $\{10^{-2}, 10^{-3}, \dots, 10^{-8}\}$ for Adam.

optimizer	fixed parameters	searched parameters
Adam	$(\eta_0, \beta_1, \beta_2)$ = (0.001, 0.9, 0.999)	$\epsilon \in \{10^{-2}, 10^{-3}, \dots, 10^{-8}\}$
Adam*	$(\eta_0, \beta_1, \beta_2, \epsilon)$ = (0.001, 0.9, 0.999, 10^{-5})	
SET-Adam (w. o. down-translating)	$(\eta_0, \beta_1, \beta_2, \epsilon, \tau)$ = (0.001, 0.9, 0.999, 10^{-5} , 0.0)	
SET-Adam	$(\eta_0, \beta_1, \beta_2, \epsilon, \tau)$ = (0.001, 0.9, 0.999, 10^{-5} , 0.5)	

APPENDIX D
PROOF OF THEOREM 1

Proof. Firstly, we note that the first bias term $1 - \beta_1^t$ in the update expressions of SET-Adam in Algorithm 1 can be absorbed into the common stepsize η_t . Therefore, we will ignore the first bias term in the following proof. Suppose $\boldsymbol{\theta}^*$ is the optimal

solution for solving the convex optimization problem, i.e., $\theta^* = \arg \min_{\theta} f(\theta)$. Using the fact that $\theta_t = \theta_{t-1} - \eta_t \tilde{w}_t^{-1} m_t$, we have

$$\begin{aligned}
& \|\tilde{w}_t^{1/2}(\theta_t - \theta^*)\|_2^2 \\
&= \|\tilde{w}_t^{1/2}(\theta_{t-1} - \eta_t \tilde{w}_t^{-1} m_t - \theta^*)\|_2^2 \\
&= \|\tilde{w}_t^{1/2}(\theta_{t-1} - \theta^*)\|_2^2 + \eta_t^2 \|\tilde{w}_t^{-1/2} m_t\|_2^2 \\
&\quad - 2\eta_t \langle \beta_{1t} m_{t-1} + (1 - \beta_{1t}) g_t, \theta_{t-1} - \theta^* \rangle \\
&= \|\tilde{w}_t^{1/2}(\theta_{t-1} - \theta^*)\|_2^2 + \eta_t^2 \|\tilde{w}_t^{-1/2} m_t\|_2^2 \\
&\quad - 2\eta_t (1 - \beta_{1t}) \langle g_t, \theta_{t-1} - \theta^* \rangle - 2\eta_t \beta_{1t} \langle m_{t-1}, \theta_{t-1} - \theta^* \rangle \\
&\leq \|\tilde{w}_t^{1/2}(\theta_{t-1} - \theta^*)\|_2^2 + \eta_t^2 \|\tilde{w}_t^{-1/2} m_t\|_2^2 \\
&\quad - 2\eta_t (1 - \beta_{1t}) \langle g_t, \theta_{t-1} - \theta^* \rangle \\
&\quad + \eta_t^2 \beta_{1t} \|\tilde{w}_t^{-1/2} m_{t-1}\|_2^2 + \beta_{1t} \|\tilde{w}_t^{1/2}(\theta_{t-1} - \theta^*)\|_2^2,
\end{aligned} \tag{14}$$

where the above inequality uses the Cauchy-Schwartz inequality $2\langle a, b \rangle \leq \|a\|_2^2 + \|b\|_2^2$. Note that (14) corresponds to (2) in the appendix of [22] for AdaBelief.

Summing (14) from $t = 1$ until $t = T$, rearranging the quantities, and exploiting the property that $g_t = \nabla f(\theta_{t-1})$ and $f(\cdot)$ being convex gives

$$\begin{aligned}
& f(\bar{\theta}_T) - f(\theta^*) \\
&= f\left(\frac{1}{T} \sum_{t=0}^{T-1} \theta_t\right) - f(\theta^*) \\
&\stackrel{(a)}{\leq} \frac{1}{T} \sum_{t=1}^T (f(\theta_{t-1}) - f(\theta^*)) \\
&\stackrel{(b)}{\leq} \frac{1}{T} \sum_{t=1}^T \langle g_t, \theta_{t-1} - \theta^* \rangle \\
&\leq \frac{1}{T} \sum_{t=1}^T \left[\frac{1}{2\eta_t(1 - \beta_{1t})} \left(\|\tilde{w}_t^{1/2}(\theta_{t-1} - \theta^*)\|_2^2 - \|\tilde{w}_t^{1/2}(\theta_t - \theta^*)\|_2^2 \right) \right. \\
&\quad \left. + \frac{\eta_t}{2(1 - \beta_{1t})} \|\tilde{w}_t^{-1/2} m_t\|_2^2 + \frac{\eta_t \beta_{1t}}{2(1 - \beta_{1t})} \|\tilde{w}_t^{-1/2} m_{t-1}\|_2^2 + \frac{\beta_{1t}}{2\eta_t(1 - \beta_{1t})} \|\tilde{w}_t^{1/2}(\theta_{t-1} - \theta^*)\|_2^2 \right] \\
&\stackrel{\beta_{11}=\beta_1}{\leq} \frac{1}{2\eta(1 - \beta_1)T} \|\tilde{w}_1^{1/2}(\theta_0 - \theta^*)\|_2^2 \\
&\quad + \frac{1}{T} \sum_{t=1}^{T-1} \left(\frac{1}{2\eta_{t+1}(1 - \beta_{1(t+1)})} \|\tilde{w}_{t+1}^{1/2}(\theta_t - \theta^*)\|_2^2 - \frac{1}{2\eta_t(1 - \beta_{1t})} \|\tilde{w}_t^{1/2}(\theta_t - \theta^*)\|_2^2 \right) \\
&\quad + \frac{1}{T} \sum_{t=1}^T \left[\frac{\eta_t}{2(1 - \beta_{1t})} \|\tilde{w}_t^{-1/2} m_t\|_2^2 + \frac{\eta_t \beta_{1t}}{2(1 - \beta_{1t})} \|\tilde{w}_t^{-1/2} m_{t-1}\|_2^2 + \frac{\beta_{1t}}{2\eta_t(1 - \beta_{1t})} \|\tilde{w}_t^{1/2}(\theta_{t-1} - \theta^*)\|_2^2 \right] \\
&\quad \left(\text{condition: } \begin{cases} 0 \leq \tilde{w}_t[i] \leq \tilde{w}_{t-1}[i] \text{ for all } i = 1, \dots, d, \\ 0 \leq \eta_t \leq \eta_{t-1}, 0 \leq \beta_{1(t+1)} \leq \beta_{1t} < 1 \end{cases} \right) \\
&\leq \frac{1}{2\eta(1 - \beta_1)T} \|\tilde{w}_1^{1/2}(\theta_0 - \theta^*)\|_2^2 \\
&\quad + \frac{1}{T} \sum_{t=1}^{T-1} \left(\frac{1}{2\eta_{t+1}(1 - \beta_{1t})} \|\tilde{w}_{t+1}^{1/2}(\theta_t - \theta^*)\|_2^2 - \frac{1}{2\eta_t(1 - \beta_{1t})} \|\tilde{w}_t^{1/2}(\theta_t - \theta^*)\|_2^2 \right) \\
&\quad + \frac{1}{T} \sum_{t=1}^T \left[\frac{\eta_t}{2(1 - \beta_1)} \|\tilde{w}_{t+1}^{-1/2} m_t\|_2^2 + \frac{\eta_t \beta_1}{2(1 - \beta_1)} \|\tilde{w}_t^{-1/2} m_{t-1}\|_2^2 + \frac{\beta_{1t}}{2\eta_t(1 - \beta_1)} \|\tilde{w}_t^{1/2}(\theta_{t-1} - \theta^*)\|_2^2 \right]
\end{aligned}$$

$$\begin{aligned}
& \text{(condition: } 0 \leq \eta_t \leq \eta_{t-1}, \mathbf{m}_0 = \mathbf{0} \text{)} \\
& \leq \frac{1}{2\eta(1-\beta_1)T} \|\tilde{\mathbf{w}}_1^{1/2}(\boldsymbol{\theta}_0 - \boldsymbol{\theta}^*)\|_2^2 + \frac{1}{T} \sum_{t=1}^{T-1} \frac{1/\eta_{t+1} - 1/\eta_t}{2(1-\beta_1)} \|\tilde{\mathbf{w}}_{t+1}^{1/2}(\boldsymbol{\theta}_t - \boldsymbol{\theta}^*)\|_2^2 \\
& \quad + \frac{1}{T} \sum_{t=1}^T \frac{\eta_t(1+\beta_1)}{2(1-\beta_1)} \|\tilde{\mathbf{w}}_{t+1}^{-1/2} \mathbf{m}_t\|_2^2 + \frac{1}{T(1-\beta_1)} \sum_{t=1}^T \frac{\beta_{1t}}{2\eta_t} \|\tilde{\mathbf{w}}_t^{1/2}(\boldsymbol{\theta}_{t-1} - \boldsymbol{\theta}^*)\|_2^2 \\
& \text{(condition: } \|\boldsymbol{\theta}^*\|_\infty \leq D, \|\boldsymbol{\theta}_t\|_\infty \leq D \text{)} \\
& \leq \frac{2D^2}{\eta(1-\beta_1)T} \sum_{i=1}^d (\tilde{\mathbf{w}}_1[i]) + \frac{2D^2}{T(1-\beta_1)} \sum_{t=1}^{T-1} (1/\eta_{t+1} - 1/\eta_t) \sum_{i=1}^d \tilde{\mathbf{w}}_t[i] \\
& \quad + \frac{1}{T} \sum_{t=1}^T \frac{\eta_t(1+\beta_1)}{2(1-\beta_1)} \|\tilde{\mathbf{w}}_{t+1}^{-1/2} \mathbf{m}_t\|_2^2 + \frac{2D^2}{T(1-\beta_1)} \sum_{t=1}^T \frac{\beta_{1t}}{\eta_t} \sum_{i=1}^d \tilde{\mathbf{w}}_t[i] \\
& \stackrel{(c)}{\leq} \frac{2D^2 d(G_\infty + \sqrt{\epsilon})}{\eta(1-\beta_1)T} + \frac{2D^2(G_\infty + \sqrt{\epsilon})d}{\sqrt{T}(1-\beta_1)\eta} + \frac{1}{T} \sum_{t=1}^T \frac{\eta_t(1+\beta_1)}{2(1-\beta_1)} \|\tilde{\mathbf{w}}_{t+1}^{-1/2} \mathbf{m}_t\|_2^2 + \frac{2D^2 \beta_1(G_\infty + \sqrt{\epsilon})d}{T(1-\beta_1)\eta(1-\lambda)^2}, \tag{15}
\end{aligned}$$

where both step (a) and (b) use the property of $f(\cdot)$ being convex, and step (c) uses the following conditions

$$\begin{cases} \|\mathbf{g}_t\|_\infty \leq G_\infty \sqrt{1-\beta_2} \Rightarrow \|\mathbf{v}_t\|_\infty \leq G_\infty^2(1-\beta_2) \Rightarrow \|\tilde{\mathbf{w}}_t\|_\infty \leq \sqrt{G_\infty^2 + \epsilon} \Rightarrow \|\tilde{\mathbf{w}}_t\|_\infty \leq G_\infty + \sqrt{\epsilon} \\ \sum_{t=1}^{T-1} (1/\eta_{t+1} - 1/\eta_t) = \frac{1}{\eta} \sum_{t=1}^{T-1} (\sqrt{t+1} - \sqrt{t}) \leq \sqrt{T}/\eta \\ \sum_{t=1}^T \frac{\beta_{1t}}{\eta_t} \leq \frac{\beta_1}{\eta} \sum_{t=1}^T \lambda^{t-1} \sqrt{t} \leq \frac{\beta_1}{\eta} \sum_{t=1}^T \lambda^{t-1} t \leq \frac{\beta_1}{\eta(1-\lambda)^2}. \end{cases} \tag{16}$$

Next we consider the quantity $\sum_{t=1}^T \eta_t \|\tilde{\mathbf{w}}_{t+1}^{-1/2} \mathbf{m}_t\|_2^2$ in (15), the upper bound of which can be derived in the same manner as Equ. (4) in the appendix of [22]:

Lemma 1. Let $\mathbf{g}_{1:T}^2[i] = ((\mathbf{g}_1[i])^2, \dots, (\mathbf{g}_T[i])^2) \in \mathbb{R}^T$. Under the three assumptions given in the theorem, we have

$$\sum_{t=1}^T \eta_t \|\tilde{\mathbf{w}}_{t+1}^{-1/2} \mathbf{m}_t\|_2^2 \leq \frac{\eta \sqrt{1 + \log T}}{\sqrt{c}(1-\beta_1)^2} \|\mathbf{g}_{1:T}^2[i]\|_2. \tag{17}$$

Finally, plugging (17) into (15) produces the upper-bound regret in the theorem. The proof is complete. \square

APPENDIX E

PARAMETER-SETUPS FOR TRAINING DIFFERENT DNN MODELS

TABLE VI
PARAMETER-SETUPS FOR TRAINING RESNET18 OVER IMAGENET. wd IN THE TABLE REFERS TO THE WEIGHT-DECAY PARAMETER.

optimizer	fixed parameters	searched parameters
AdaBelief	$(\eta_0, \beta_1, \beta_2, wd)$ $= (0.001, 0.9, 0.999, 10^{-2})$	$\epsilon \in \{10^{-8}, 10^{-9}, 10^{-10}\}$
Adam	$(\eta_0, \beta_1, \beta_2)$ $= (0.001, 0.9, 0.999)$	$\epsilon \in \{10^{-3}, 10^{-8}\}$ $wd \in \{10^{-2}, 10^{-5}\}$
SET-Adam	$(\eta_0, \beta_1, \beta_2, \epsilon, \tau, wd)$ $= (0.001, 0.9, 0.999, 10^{-6}, 0.5, 10^{-2})$	

TABLE VII
PARAMETER-SETUPS FOR TRAINING A TRANSFORMER. THE WEIGHT DECAY FOR ADAMW WAS SET TO $5e-4$ WHILE THE WEIGHT DECAY FOR ALL OTHER ALGORITHMS WAS SET TO 0.0.

optimizer	fixed parameters	searched parameters
AdaBound	$(\eta_0, \beta_1, \beta_2, \gamma) = (0.001, 0.9, 0.98, 0.001)$	$\epsilon \in \{1e-6, 1e-7, \dots, 1e-12\}$ final_stepsize $\in \{0.1, 0.01, 0.001\}$
Yogi	$(\eta_0, \beta_1, \beta_2) = (0.001, 0.9, 0.98)$	$\epsilon \in \{1e-2, 1e-3, \dots, 1e-8\}$
SGD	momentum=0.9	$\eta_0 \in \{1.0, 0.1, 0.01, 0.001\}$
RAdam	$(\eta_0, \beta_1, \beta_2) = (0.001, 0.9, 0.98)$	$\epsilon \in \{1e-6, 1e-7, \dots, 1e-12\}$
MSVAG	$(\eta_0, \beta_1, \beta_2) = (0.001, 0.9, 0.98)$	$\epsilon \in \{1e-6, 1e-7, \dots, 1e-12\}$
Fromage		$\eta_0 \in \{0.1, 0.01, 0.001, 0.0001\}$
Adam	$(\eta_0, \beta_1, \beta_2) = (0.001, 0.9, 0.98)$	$\epsilon \in \{1e-6, 1e-7, \dots, 1e-12\}$
AdamW	$(\eta_0, \beta_1, \beta_2) = (0.001, 0.9, 0.98)$	$\epsilon \in \{1e-6, 1e-7, \dots, 1e-12\}$
AdaBelief	$(\eta_0, \beta_1, \beta_2) = (0.001, 0.9, 0.98)$	$\epsilon \in \{1e-8, 1e-10, \dots, 1e-16\}$
SET-Adam(our)	$(\eta_0, \beta_1, \beta_2, \epsilon, \tau) = (0.001, 0.9, 0.98, 1e-15, 0.5)$	

TABLE VIII
PARAMETER-SETUPS FOR TRAINING LSTMS. THE WEIGHT DECAY FOR EVERY ALGORITHM WAS SET TO $1.2e-6$.

optimizer	fixed parameters	searched parameters
AdaBound	$(\beta_1, \beta_2, \gamma) = (0.9, 0.999, 0.001)$	$\eta_0 \in \{0.01, 0.001\}$ $\epsilon \in \{1e-6, 1e-8, \dots, 1e-12\}$ final_stepsize $\in \{0.1, 3, 30\}$
Yogi	$(\beta_1, \beta_2) = (0.9, 0.999)$	$\eta_0 \in \{0.01, 0.001\}$ $\epsilon \in \{1e-2, 1e-3, 1e-4, 1e-5\}$
SGD	momentum=0.9	$\eta_0 \in \{30, 3, 1, 0.1\}$
RAdam	$(\beta_1, \beta_2) = (0.9, 0.999)$	$\eta_0 \in \{0.01, 0.001\}$ $\epsilon \in \{1e-6, 1e-8, 1e-10, 1e-12\}$
MSVAG	$(\beta_1, \beta_2) = (0.9, 0.999)$	$\eta_0 \in \{30, 1, 0.01, 0.001\}$ $\epsilon \in \{1e-6, 1e-8, 1e-10, 1e-12\}$
Fromage		$\eta_0 \in \{0.1, 0.01, 0.001\}$
Adam	$(\beta_1, \beta_2) = (0.9, 0.999)$	$\eta_0 \in \{0.01, 0.001\}$ $\epsilon \in \{1e-6, 1e-8, 1e-10, 1e-12\}$
AdamW	$(\beta_1, \beta_2) = (0.9, 0.999)$	$\eta_0 \in \{0.01, 0.001\}$ $\epsilon \in \{1e-6, 1e-8, 1e-10, 1e-12\}$
AdaBelief	$(\beta_1, \beta_2) = (0.9, 0.999)$	$\eta_0 \in \{0.01, 0.001\}$ $\epsilon \in \{1e-8, 1e-10, \dots, 1e-16\}$
SET-Adam(our) [for layer 1 and 2]	$(\eta_0, \beta_1, \beta_2, \epsilon, \tau) = (0.001, 0.9, 0.999, 1e-13, 0.5)$	
SET-Adam(our) [for layer 3]	$(\eta_0, \beta_1, \beta_2, \epsilon, \tau) = (0.001, 0.9, 0.999, 1e-11, 0.5)$	

TABLE IX
PARAMETER-SETUPS FOR TRAINING WGAN-GP. THE WEIGHT DECAY FOR ADAMW WAS SET TO $5e-4$ WHILE THE WEIGHT DECAY FOR ALL OTHER ALGORITHMS WAS SET TO 0.0.

optimizer	fixed parameters	searched parameters
AdaBound	$(\eta_0, \beta_1, \beta_2, \gamma) = (0.0002, 0.5, 0.999, 0.001)$	$\epsilon \in \{1e-2, 1e-4, \dots, 1e-10\}$ final_stepsize $\in \{0.1, 0.01\}$
Yogi	$(\eta_0, \beta_1, \beta_2) = (0.0002, 0.5, 0.999)$	$\epsilon \in \{1e-2, 1e-3, 1e-4, 1e-5\}$
SGD		momentum = $\{0.3, 0.5, 0.9\}$ $\eta_0 \in \{0.1, 0.02, 0.002, 0.0002\}$
RAdam	$(\eta_0, \beta_1, \beta_2) = (0.0002, 0.5, 0.999)$	$\epsilon \in \{1e-4, 1e-6, \dots, 1e-14\}$
MSVAG	$(\beta_1, \beta_2) = (0.5, 0.999)$	$\eta_0 \in \{0.1, 0.02, 0.002, 0.0002\}$ $\epsilon \in \{1e-4, 1e-6, \dots, 1e-14\}$
Fromage		$\eta_0 \in \{0.1, 0.01, 0.001\}$
Adam	$(\eta_0, \beta_1, \beta_2) = (0.0002, 0.5, 0.999)$	$\epsilon \in \{1e-4, 1e-6, \dots, 1e-14\}$
AdamW	$(\eta_0, \beta_1, \beta_2) = (0.0002, 0.5, 0.999)$	$\epsilon \in \{1e-4, 1e-6, \dots, 1e-14\}$
AdaBelief	$(\eta_0, \beta_1, \beta_2, \epsilon) = (0.0002, 0.5, 0.999, 1e-12)$	
SET-Adam(our)	$(\eta_0, \beta_1, \beta_2, \epsilon, \tau) = (0.0002, 0.5, 0.999, 1e-11, 0.5)$	

TABLE X
PARAMETER-SETUPS FOR TRAINING VGG AND RESNET MODELS OVER CIFAR10 AND CIFAR100. THE WEIGHT DECAY FOR ADAMW WAS SET TO 0.01 WHILE THE WEIGHT DECAY FOR ALL OTHER ALGORITHMS WAS SET TO $5e-4$.

optimizer	fixed-parameters	searched-parameters
AdaBound	$(\eta_0, \beta_1, \beta_2, \gamma) = (0.001, 0.9, 0.999, 0.001)$	$\epsilon \in \{1e-2, 1e-3, \dots, 1e-8\}$ final_stepsize $\in \{0.1, 0.01\}$
Yogi	$(\eta_0, \beta_1, \beta_2,) = (0.001, 0.9, 0.999)$	$\epsilon \in \{1e-1, 1e-2, 1e-3\}$
SGD	(momentum, η_0) = (0.9, 0.1)	
RAdam	$(\eta_0, \beta_1, \beta_2) = (0.001, 0.9, 0.999)$	$\epsilon \in \{1e-2, 1e-3, \dots, 1e-8\}$
MSVAG	$(\eta_0, \beta_1, \beta_2) = (0.1, 0.9, 0.999)$	$\epsilon \in \{1e-2, 1e-2, \dots, 1e-8\}$
Fromage		$\eta_0 \in \{0.1, 0.01, 0.001\}$
Adam	$(\eta_0, \beta_1, \beta_2) = (0.001, 0.9, 0.999)$	$\epsilon \in \{1e-2, 1e-3, \dots, 1e-8\}$
AdamW	$(\eta_0, \beta_1, \beta_2) = (0.001, 0.9, 0.999)$	$\epsilon \in \{1e-2, 1e-3, \dots, 1e-8\}$
AdaBelief	$(\eta_0, \beta_1, \beta_2) = (0.001, 0.9, 0.999)$	$\epsilon \in \{1e-8, 1e-9\}$
SET-Adam (our)	$(\eta_0, \beta_1, \beta_2, \epsilon, \tau) = (0.001, 0.9, 0.999, 1e-5, 0.5)$	